FIELD MEASUREMENTS AND MODELLING OF THE TRANSIENTS PROPAGATION PROPERTIES OF A 380 KV CABLE SYSTEM OF 7.5 KM LENGTH AT BEWAG, BERLIN

M. ERMEL, J. F .NNICKE
Technische Fachhochschule Berlin
13353 Berlin
Luxemburger Straße 10

M. HENSCHEL
Berliner Kraft- und Licht (Bewag)-AG
10785 Berlin
Stauffenbergstraße 26

1. Introduction

The calculation of transient wave propagation is well established for overhead transmission lines by means of sufficient accuracy. For high-voltage cables however, there still remains a lack of correspondence between measurements and simulation results. In order to better assess the transients propagation properties of cables as well as to improve current techniques for numerical simulation of transient overvoltages, field measurements and calculations have been performed at the newly installed 380 kV cable system of the BEWAG, Berlin.

2. Description of the tested cable system

The isolated operation of West Berlin's power system of approxim. 2 GW ceased with the commissioning of a 380 kV connection to the East European interconnecting network in December 1994. The link consists of an overhead transmission line bridging a distance of 150 km between Wolmirstedt and Berlin's city limits, and an underground cable system leading from there to the generation sites downtown (Figure 1). The tested cable system of 7.5 km lenght is newly installed between the GIS stations Teufelsbruch "T" and Reuter "R" [1].

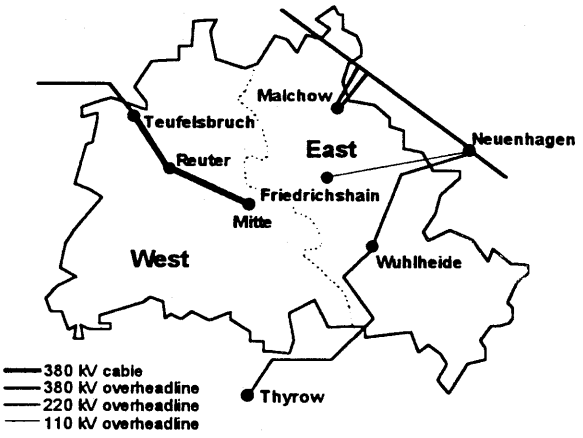

Figure 1: 380 kV cables of Berlin's power system

The cable system is made up of six parallel low-pressure, single-phase, oil-filled cables, each having a copper conductor of 1200 mm^2 (Figure 2). The conductors are enclosed in polyethylene (PE) tubes and water-cooled. The connecting cable joints rest in 18 pits. To avoid induced sheath losses, the cable jackets are cross-bonded at four locations. Each cable ends at a SF_6 switchgear unit.

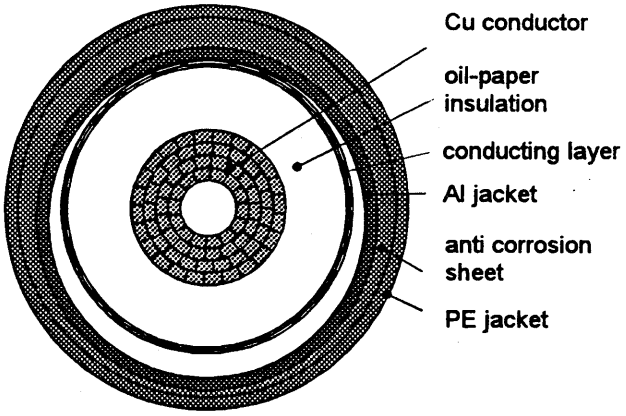

Figure 2: cross section of the invastigated cable

A recent conduct of cable load tests offered the opportunity to pursue an investigation of the transients properties of the cable and adjacent devices. From these measurements we obtained a basis for the calculation of overvoltages, specifically in terms of the characteristic impedance, propagation time, and frequency dependent damping.

3. Field measurements

Before commissioning, on-site time-domain measurements had been performed at a single-phase of the cable system in order to reveal its characteristic transmission line parameters. For this purpose, the crossbondings were removed, and the cable jackets were linked along the single-phase cable. The test setup is shown in Figure 3. Both cable ends were accessible through maintenance openings in the GIS-Cable junctions. A low voltage pulse generator of 50 Ω internal resistance had been connected to the terminal at station "T" passing a cylindrical adapter which had the same characteristic impedance as the short GIS bus duct of 84 Ω.

During the test, rectangular pulses with a pulse length of a few milliseconds, and a rise time of less than. 1 ns were injected in order to generate travelling waves The reflected signals were then recorded utilizing a500 MHz transient digitizing oscilloscope (DSO) with 1 GS/s and 50 KBytes.

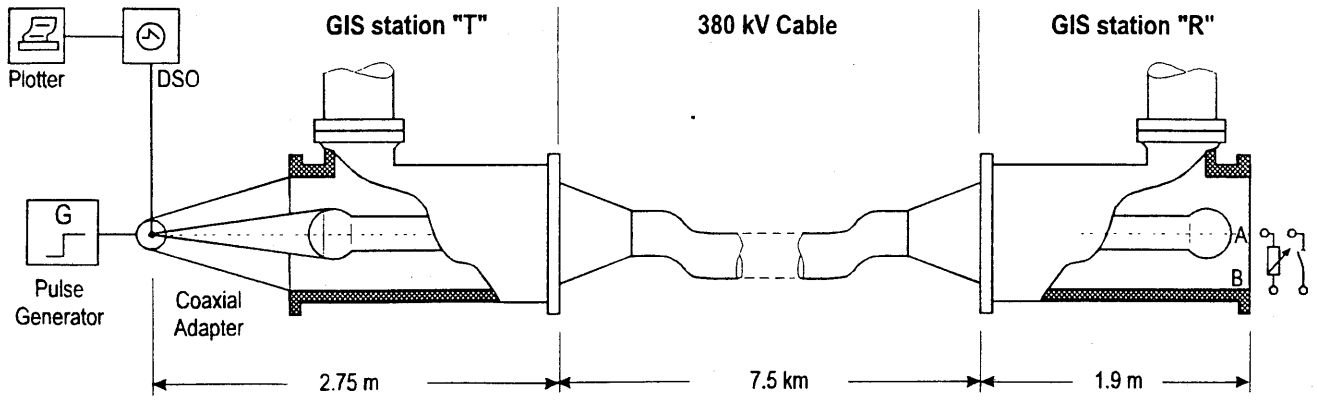

Figure 3: Test setup for the field measurements

The measurements were taken while applying one of the following three conditions to the cable terminal in station "R" (see points A and B in Figure 3) :

- open end
- shorted end
- matched end.

The transient voltage signal for the case with the short-circuited cable end is displayed in Figure 4. A voltage step of approxim. 4.1V was applied to the terminal at station "T",

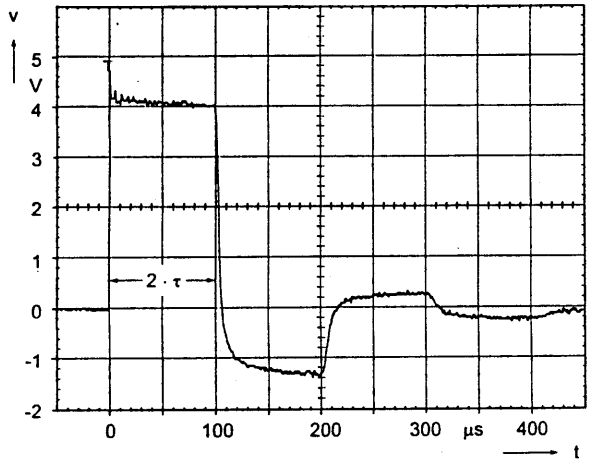

Figure 4: The measured voltage signal in case of the short-circuited cable end in station "R"

which started to propagate along the cable. After reaching the short-circuited end in station "R", the incoming travelling wave was reflected and returned to station "T", where it arrived after twice its propagation time 2τ. This caused the voltage at station "T" to collapse, which is a result of the superposition of the forward and backward travelling waves. The negative overshoot and the following reflections are caused by the mismatch in the characteristic impedances of both the pulse generator and the cable.

From Figure 4 we can read the propagation time to $\tau = 50.0$ µs. Thus, having a cable length of 7550 m, the propagation velocity is $v = 151$ m/µs. It should be noticed however, that these propagation values are valid only for a limited frequency range.

Another question of interest was how cable discontinuities, like the 18 joints along the line, would influence the transient transfer behaviour. A study of the "ripples" that appear on top of the main voltage signal during the first 100 µs reveals that the small peaks can be attributed to the 18 cable joints between the stations. Figure 5 shows the corresponding detail of Figure 4. Even a slight magnification of the peaks is sufficient to recognize at least 10 of the 18 cable joints, each being located about 400 m apart. The time intervals between the peaks can be related to the distances between the cable joints and allow their precise location with only about ±1% uncertainty.

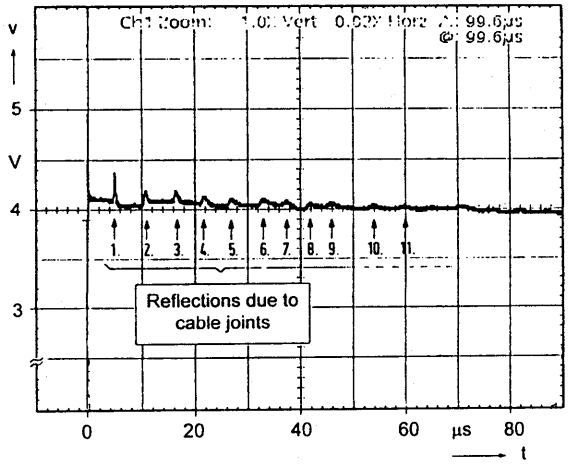

Figure 5: Reflections due to cable joints (magnified detail of Figure 4)

The first peak on top of the voltage step is a result of the discontinuity between the pulse generator (50 Ω), the short coaxial adapter and bus duct (84 Ω), and the entire cable with its characteristic impedance. The initial pulse thus generates several travelling waves in that section; however it can be found, that their impact to the

relevant voltage signal becomes negligible as they cease within about 0.1 μs after the pulse injection.

In order to determine the characteristic cable impedance on-site, a variable pure ohmic resistor was connected to the cable end A-B at Station "R", and adjusted until no reflections occured. Then, the characteristic impedance Z was read to 26.0 Ω.

As a confirmation of the said results, all measurements were additionally performed under open end condition in station "R". The measured voltage signals differ, as expected, from the signals under shorted end condition. Nevertheless, the evaluation yield the same characteristic cable parameters, thus, confirming the results.

An additional on-site measurement was performed to evaluate the damping coefficient of the cable. For this test, the pulse generator was removed from the measuring point. Thus, the cable termination at station "T" became open-ended or nearly open-ended if the impact of the high impedance voltage probe was to be taken into account. The cable was then charged with 8V DC and short-circuited at the cable termination A-B in station "R" (see Figure 3). Figure 6a shows the voltage signal at station "T", which results from the superposition of travelling waves between the open and the short-circuited end of the cable. This measurement is further discussed in Chapter 5.

4. Simulations

Numerical simulations were carried out using the Electromagnetic Transients Program EMTP [2]. The input data were obtained from manufacturing documents and cable measurements, as well as from previous tests and calculations based on the cable geometry.

The program provides access to three different types of transmission line models:

- a distortionless line model
- a line model by SEMLYEN
- a line model by MARTI.

In comparison to the distortionless line model, the two other models take the frequency dependent damping of travelling waves into account. However, both models differ in the approximation of the transfer function: while SEMLYEN's line model allows only two exponential functions for the approximation, the model by MARTI is, in theory, not at all limited to any particular number of exponential functions; yet it requires the number to be explicitly defined. In our simulation runs, we specified this number with 20 exponential functions [3]. Using less than 20 exponential functions at a given accuracy of one percent, we experienced convergence difficulties of the simulation.

5. Comparison of test and simulation results

Generating travelling waves by shorting a charged cable at one end, as described in Chapter 3, appeared to be most advantageous for a comparison between measurement and simulation.

Figure 6 shows both the measured voltage signal(6a) and the simulation result (6b) using the three different EMTP cable models as explained in Chapter 4.

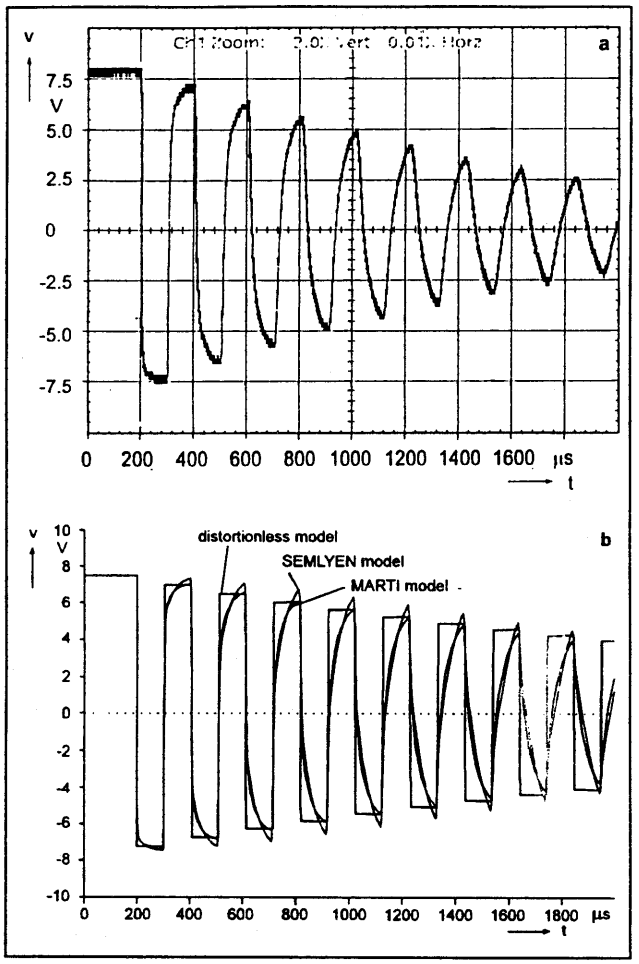

Figure 6: Travelling waves by shorting the charged cable: a) measurement, b) simulations

From Figure 6 it appears that the simulation results of the two models by SEMLYEN and MARTI agree with the measured curve which can be explained by the frequency dependence of both models. Notice that the simulation with SEMLYEN's model shows magnitudes that are slightly higher than the ones of the two other models, which is a result of using only two exponential functions to account for the transfer function. Of all three different types, MARTI's model best corresponds with the measured signal. However, a closer look at the graphs, as it is shown in Figure 7, discloses that all three simulations considerably differ from the measured curve.

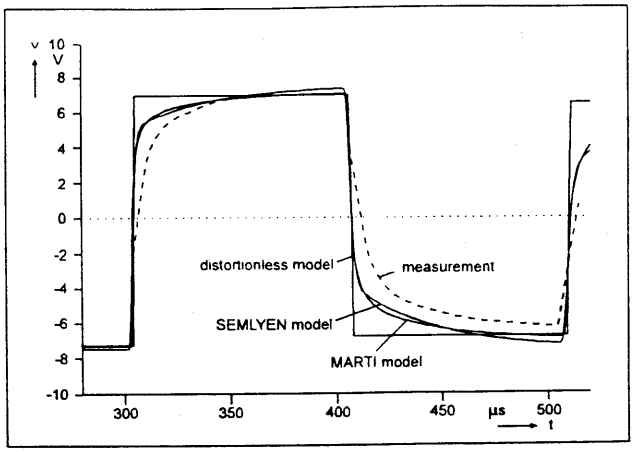

Figure 7: Comparison of test and simulation results

It seems that the modelled transfer functions are not sufficiently damped. The problems of unsufficent correspondence between test and simulation results may be due to our restrictions by using only the EMTP-Cable Constants Module. At this point, it has been suggested to identify the parameters of the transfer function from the measured graphs, as described in [4].

Even though the difference may seem significant, we find that the simulation results still are of high practical value for the computation of transient overvoltages.

Considering a larger time span, it becomes apparent that the overall damping effect is higher in the measured transients than in the simulated graphs which, indeed, is a common phenomenon in practice. After 2 ms the measured voltage signal has decreased to 33 % of its initial value, whereas the simulated curves still maintain a value of 49 %. Hence, the simulation provides a safety margin in regard of the results.

Table I: Characteristic cable parameters

Cable constants	measured	calculated
Capacitance C' / µF/km	0.291	0.266
Inductance L' / mH/km	N/A	0.169
Propagation time τ / µs	50.0	50.6
Characteristic impedance Z / Ω	26.0	25.3
Damping coefficient δ / s^{-1}	667	400
Decay time T / ms	1.5	2.5
Propagation velocity v / $m.\mu s^{-1}$	151	149

Table I shows the characteristic propagation parameters of the cable, as they were obtained through our measurements and calculations.

6. Effect of crossbonding

Under normal operation conditions, the cable jackets are usually crossbonded and grounded as shown in Figure 8. In addition, surge arresters have been installed at the crossbonding points to protect the cable jackets against induced overvoltages. The surge arresters are rated at a voltage of 4.5 kV and have a residual voltage of 10 kV at a surge current of 10 kA.

In order to study the effect of crossbonding, we simulated the entire three-phase system as shown in Figure 8. Travelling waves were generated by shorting the energised cable system in station "R" at phase L1. The cable terminals in station "T" were presumed to be open-ended. The cable system was simulated by seven-three-phase MARTI's transmission line models. Models of the surge arresters were connected to the cable jacket sections wherever there was no ground connection.

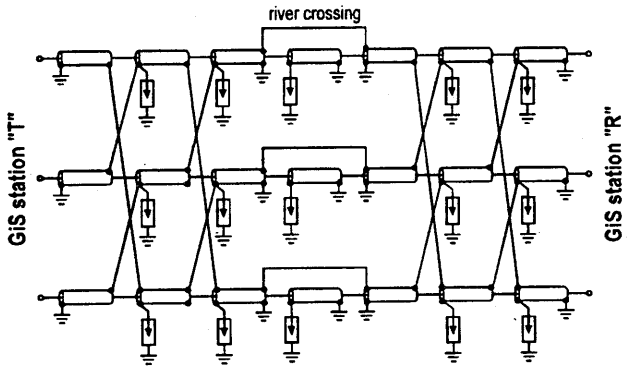

Figure 8: Crossbonding system on both sides of a river crossing

In this simulation case, the transient voltages at the open cable terminals in station "T" were of particular interest (Figure 9). It is obvious that now, including the crossbondings in our simulation, we would obtain different results than with the measurements in Chapter 5.

Additional simulations revealed that the travelling waves in the cable generated overvoltages in the jacket that were so high that the surge arresters respond (Figure 9b). Therefore, the entire cable jacket was kept near ground potential which, in fact, is the same as if there were not existing crossbondings at all.

It can be found that during a transient period, a certain amount of system energy is being dissipated through the surge arresters. Thus, the system is highly damped and, after less than three reflections, returns to its 50 Hz base frequency. Hence, it can be concluded that the protection mechanisms of the system provide sufficient security against high overvoltages.

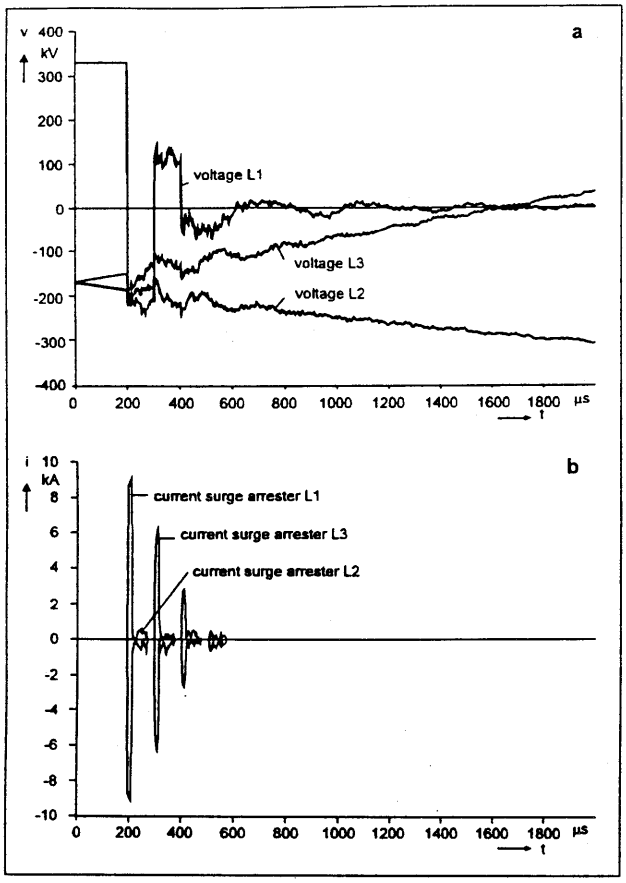

Figure 9: Single-phase fault in station "R"
a) transient voltages at the open end in "T"
b) Currents through the surge arresters

7. Summary

The transient propagation properties were investigated at the newly installed 380 kV cable system of the Bewag, Berlin. Field measurements and numerical simulations are compared.

The measurements on-site were performed with low voltage travelling waves at a single-phase cable, the crossbondings disabled. The measurement technique is relatively uncomplicated and easy to conduct. The evaluation yields the characteristic impedance, propagation time and velocity, and damping behaviour, as listed in Table I.

The simulations were carried out using EMTP with the Cable Constance Module for data input. Three implemented line models were used and compared: the distortionless, SEMILYEN's, and MARTI's line model. As a result of comparison, MARTI's model best corresponds with the measured transient signal. However a lack of correspondence remains in the damping behaviour. The measured damping was found to be always higher than the computed one. It was not possible to achieve a better curve-fitting by using the Cable Constance Module.

Considering the computation of transient overvoltages, the effect of a smaller damping in the numerical simulations provides a safety margin, and the simulation results still are of high practical value.

Finally, the transient phenomena with the crossbondings enabled were studied by numerical simulation. The entire three-phase cable system including the cable jacket arresters was simulated, using MARTI's transmission line models for all cable sections. It can be found that the crossbonding leads to overvoltages between the cable jackets and ground which trigger the responding of the surge arresters. This causes the jackets to be bonded to ground with the same effect as if the crossbonding would be disabled. However, a much higher damping can be observed which is due to the additional energy dissipation in the surge arresters.

References

[1] D. Hecklau, L. Hänisch, R. Schroth: Die Errichtung des 380-kV-Hochleitungskabelsystems für den Verbundanschluß der Bewag (Elektrizitätswirtschaft 94 (1995), H. 12)

[2] F. Grogger, D. van Dommelen, B. Stein. Das Programmsystem EMTP zur Berechnung elektromagnetischer- und mechanischer Ausgleichsvorgänge, e & i, Jahrgang 105, Heft 12, S. 568-573

[3] H. W. Dommel: EMTP Theory Book, Bonneville Power Administration, Portland, 1986

[4] H. J. Hinrichs: Erstellung von Simulations-Modellen basierend auf Feldtests und Parameteridentifizierung (Elektrie 47 (1993) 9, S. 351-357)